Results from Low-Energy Neutrino Searches for Dark Matter in the Galactic Center with IceCube-DeepCore

THE ICECUBE COLLABORATION[1],

[1] *See special section in these proceedings*

martin.wolf@fysik.su.se

Abstract: The cubic-kilometer sized IceCube neutrino observatory, constructed in the glacial ice at the South Pole, offers new opportunities for neutrino physics with its in-fill array “DeepCore”. In particular, the use of the outer layers of the IceCube detector as a veto allows low-energy neutrino searches to be performed in the southern sky. This makes the Galactic Center, an important target in searches for self-annihilating dark matter, reachable for IceCube. In this contribution we present the results of the first Galactic Center analysis using more than 10 months of data taken with the 79-string configuration of IceCube-DeepCore, with a special focus on low WIMP masses reaching a sensitivity as low as 30 GeV. We also present the status of an analysis extending the sensitivity to WIMP masses up to the TeV scale.

Corresponding authors:
Martin Wolf[1], Samuel Flis[1], Matthias Danninger[1], Martin Bissok[2]

[1] *Oskar Klein Centre and Dept. of Physics, Stockholm University, SE-10691 Stockholm, Sweden*
[2] *III. Physikalisches Institut, RWTH Aachen University, D-52056 Aachen, Germany*

Keywords: Dark Matter, WIMP, Galactic Center, IceCube, DeepCore.

1 Introduction

Numerous observations imply the existence of non-baryonic cold dark matter through its gravitational interaction [1]. However, the exact nature of dark matter is still unknown. Many theories beyond the Standard Model predict stable or extremely long-lived particles that are well-motivated dark matter candidates. Weakly Interacting Massive Particles (WIMPs) are one of the most promising and experimentally accessible classes of dark matter. In super-symmetric extensions to the Standard Model, WIMPs may appear in the form of neutralinos [2]. Predicted WIMP masses range from a few GeV to a few tens of TeV. WIMP self-annihilation to Standard Model particles may produce a flux of final-state particles that include positrons, gammas, or neutrinos.

Regions of increased dark matter density are interesting from an observational point of view since the ensuing higher self-annihilation rate could result in a significant flux of detectable particles. Galaxies are believed to be embedded in halos of dark matter with a variety of models attempting to describe the density distribution, based on *e.g.* N-body simulations or observations of the motion of stars within galaxies or individual galaxies within clusters of galaxies. These models, usually assume a spherically symmetric halo where the density decreases with the distance, r, from the Galactic Center.

Observations of low surface brightness galaxies suggest a flat distribution in the central region [3], while fits to N-body simulations tend to show a divergent, or cusped behavior towards the center [4]. However, at large distances from the Galactic Center($\simeq 8.5$ kpc), the different models converge. A broad family of dark matter density profiles may be parametrized by [5]

$$\rho_{\rm DM}(r) = \frac{\rho_0}{\left(\frac{r}{r_s}\right)^{\gamma} \cdot \left(1 + \left(\frac{r}{r_s}\right)^{\alpha}\right)^{(\beta-\gamma)/\alpha}}, \qquad (1)$$

where r_s is the scale radius, α, β, and γ are profile parameters, and ρ_0 is the normalization. For the analyses presented here, the Navarro-Frenk-White (NFW) model [6] is used as a benchmark. It is obtained from equation 1 with the parameters $\alpha = 1, \beta = 3, \gamma = 1, r_s = 20$ kpc, and ρ_0 chosen so that the local dark matter density $\rho(R_{\rm SC}) = 0.3$ GeVcm^{-3}, where $R_{\rm SC} = 8.5$ kpc is the radius of the solar orbit.

Searching for dark matter self-annihilation in the Milky Way probes the thermal average of the annihilation rate, which is proportional to the product of the annihilation cross section and the relative velocity of WIMPs, $\langle\sigma_A v\rangle$. This is complementary to indirect Solar and Earth WIMP searches, and to direct searches, which probe the WIMP-nucleon cross-section.

The expected flux of the annihilation products depends on the integrated dark matter density squared along the line of sight, given by [7]

$$J_a(\Psi) = \int_0^{l_{max}} \mathrm{d}l \, \frac{\rho^2_{\rm DM}(\sqrt{R^2_{\rm SC} - 2lR_{\rm SC}\cos\Psi + l^2})}{R_{\rm SC}\rho^2_{\rm SC}}. \qquad (2)$$

Here Ψ is the half-cone opening angle with respect to the Galactic Center, and $\rho_{\rm SC} = \rho(R_{\rm SC})$ and $R_{\rm SC}$ are scaling constants which make $J_a(\Psi)$ a dimensionless quantity. Figure 1 shows examples of $J_a(\Psi)$ for different halo models.

The expected neutrino flux at Earth is given by

$$\frac{\mathrm{d}\phi_\nu}{\mathrm{d}E} = \frac{\langle\sigma_A v\rangle}{2} J_a(\Psi) \frac{R_{\rm SC}\rho^2_{\rm SC}}{4\pi m^2_\chi} \frac{\mathrm{d}N_\nu}{\mathrm{d}E}, \qquad (3)$$

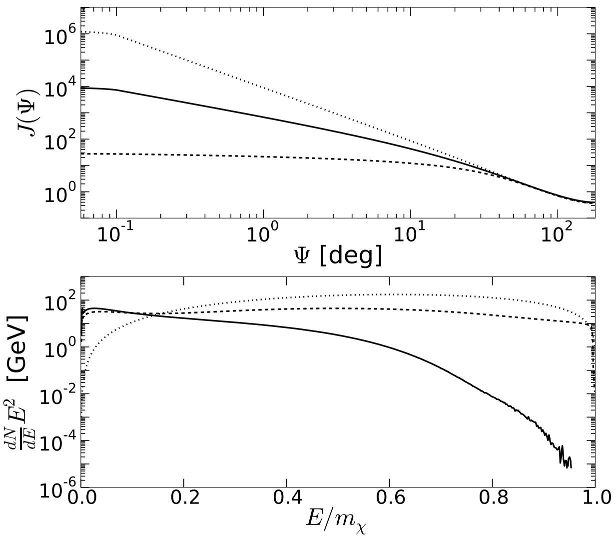

Figure 1: **Top:** Line-of-sight integral $J_a(\Psi)$ for three different models. The NFW [6] (solid) is the benchmark model for the analyses presented in this paper, Kravtsov [9] (dashed) and Moore [8] (dotted) represent more extremes cases of a flat-cored and a peaked profile. **Bottom:** Dark matter annihilation spectra generated with PYTHIA8 [10] for three channels, $b\bar{b}$ (solid), W^+W^- (dashed) and $\mu^+\mu^-$ (dotted) and a WIMP mass of $m_\chi = 500$ GeV.

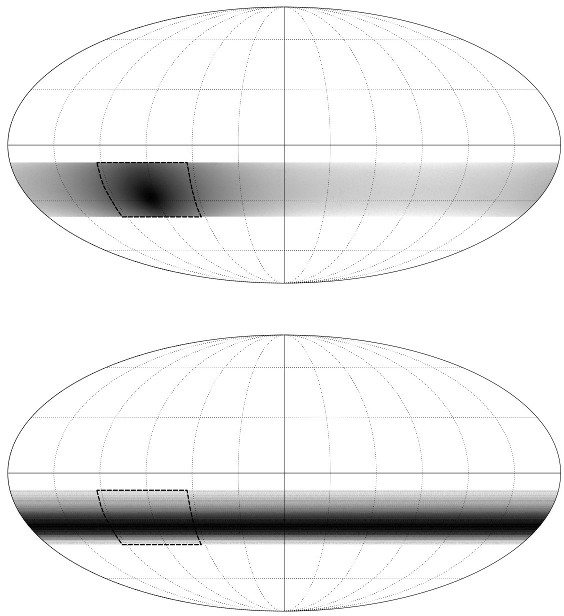

Figure 2: Signal and background skymap PDFs in equatorial coordinates for the DeepCore analysis. The search region around the Galactic Center at -29° dec. and 266° r.a. is indicated by a black dashed box. The black and white shading indicates the probability density. **Top:** Signal PDF for a 130 GeV WIMP annihilating into $\mu^+\mu^-$, assuming the NFW halo model. **Bottom:** Background PDF obtained from scrambled data.

where $\mathrm{d}N_\nu/\mathrm{d}E$ is the energy dependent WIMP annihilation spectrum, and $\rho_{\mathrm{SC}}/m_\chi$, and R_{SC} normalize $J_a(\Psi)$ to the number density. The resulting neutrino spectra from WIMP annihilations for various signal models are simulated using PYTHIA8 [10]. Figure 1 compares three such neutrino spectra. In the case of neutrinos as final-state particles, the flux from dark matter annihilations can be probed by large neutrino telescopes such as IceCube.

IceCube is a cubic-kilometer-scale neutrino detector deployed in the ice at the geographic South Pole [11] between depths of 1450 m and 2450 m. In this work we use 320 live days of data taken from 2010 to 2011, during a period when the detector was operated in its 79-string configuration, including 6 densely instrumented strings optimized for low energies in the center of the array. Together with the 7 adjacent standard IceCube strings, these form the DeepCore subarray [12]. Neutrino detection in IceCube relies on the measurement of Cherenkov radiation produced by secondary charged leptons in neutrino interactions in the surrounding ice or the nearby bedrock.

2 Event Selection

Neutrinos from the direction of the Galactic Center, located in the southern hemisphere, would be down-going events within IceCube. Searches for such neutrinos must overcome a background of down-going atmospheric muons penetrating the detector. This background is reduced by selecting events with a reconstructed interaction vertex inside a fiducial volume of the detector, where the outer parts of IceCube are used as a veto.

In order to be sensitive to a wide range of possible WIMP masses, two independent analyses are performed. The DC event selection (section 2.1) is optimized to search for low WIMP mass signals (30 GeV to 500 GeV) with DeepCore. The second search uses larger parts of IceCube as a fiducial volume to improve the sensitivity to WIMP mass signals above 500 GeV, denoted by the IC event selection (section 2.2). In order to avoid confirmation bias, the right ascension in data has been scrambled during the development of the analyses.

2.1 DC event selection

To optimize for low WIMP mass signals the bottom part of the DeepCore subarray (see also [13]) is defined as the fiducial volume. This definition includes a two-DOM thick bottom veto layer, resulting in a total fiducial volume of approximately 280 m height and 260 m width.

The event selection exclusively uses data from the DeepCore filter event stream [12]. Based on distributions of event multiplicities and observables from signal simulations and experimental data, cuts are placed to reduce the content of atmospheric muon events. This is repeated for five successive linear and one multivariate cut level. The linear cuts reduce the data rate from about 200 Hz to approximately 10 mHz. These cuts rely on the expertise from the IceCube-79 Solar WIMP analysis [14], which used DeepCore for the first time in low mass WIMP searches. In addition, they incorporate newly developed muon veto methods [13].

The last cut level is implemented using a boosted decision tree (BDT). We use the TMVA software package [15] to classify events as signal or background. Two separable classes of neutrino-induced low energy signal events were identified at the linear cut levels. The first class consists of well contained starting events within the fiducial volume, while the second is dominated by partially contained events: those that start within the fiducial volume and exit it. We therefore trained two BDTs, one for the well contained (DC-contained) and a second for partially contained (DC-partial) signal events.

The cuts on the BDT scores have been optimized for each category using the maximum likelihood method described in [14]. For the optimization of the DC-contained and DC-partial event selections the $b\bar{b}$ and W^+W^- WIMP annihilation spectra have been considered, respectively. The probability density functions (PDFs) for signal and background are constructed using healpix [16].

A box of size $-10°$ and $+20°$ in declination and $\pm30°$ in right ascension around the Galactic Center position has been used as the search region. The search region is asymmetric in declination to account for the increased background rate towards lower declination angles. The final event selection (BDT cut applied) has a data rate of approximately 1 mHz. Figure 2 shows the expected signal and background PDFs at final cut level. The background PDF is found by filling a healpix map with reconstructed declination of recorded events and scrambled right ascensions. The scrambled right ascension is found by sampling fake event times from the data-taking period. The time scramble is repeated to achieve a smooth background distribution.

Sensitivities on $\langle\sigma_A v\rangle$ are derived for each signal model for both event selections, DC-contained and DC-partial. The event selection that results in a better sensitivity for a particular signal model is used in the final analysis.

2.2 IC event selection

The search for WIMPs with masses above a few hundred GeV benefits from the large volume of IceCube in addition to DeepCore. This increase in fiducial volume comes at a cost of a smaller veto region in addition to a higher data rate.

For the IC event selection, a dedicated data pre-selection filter has been developed, which reduces the event rate from more than 2 kHz at trigger-level to about 52 Hz. Further, this search relies on a combination of three dedicated veto techniques against incoming atmospheric muon tracks.

The veto volume contains a top layer of the upper-most 200 m (equal to 12 DOM layers). In addition, a side veto is defined, that follows the hexagonal IceCube geometry and consists of two string layers. This definition of fiducial- and veto-volumes is maintained for the following veto mechanisms.

First, we demand no reconstructed interaction vertices within the top or side veto. The vertex reconstruction is based on the projection of the first hit optical modules on the reconstructed track, taking into consideration the angle of Cherenkov light emission.

The second veto does not rely on a track reconstruction, but on the causality of hit DOMs. For each event the distance in space and time is calculated for all hits in the veto region with respect to the earliest hit inside the fiducial volume, hereby omitting any coincidence cleaning for the veto hits. Faint incoming tracks produce hits in veto DOMs that are causally connected to the earliest fiducial hit. In contrast, starting tracks (signal) produce no hits within the veto region. PDFs are constructed from the number of hits, the distance in space, and distance in time, which are used for a likelihood-ratio test.

For the third veto the reconstructed arrival direction is used to calculate the point of entry of the track into

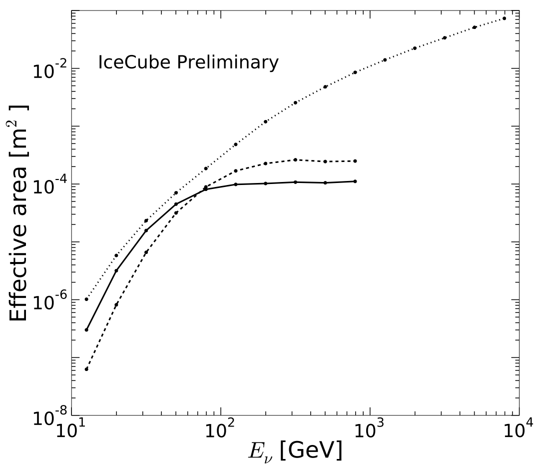

Figure 3: Neutrino effective area at analysis level for the IC event selection (dotted), the DC-contained (solid), and the DC-partial event selection (dashed).

the detector volume. The distance in the xy-plane and the signed distance along the z-axis to the earliest hit DOM is calculated. Penetrating muon background produces a distinct feature in this plane, while starting signal-like tracks do not. A box cut around this feature is applied, removing a further 50% of the background while keeping more than 99% of fiducial signal events. All three veto cuts reduce the data rate from 52 Hz to 0.45 Hz.

The final IC event selection is also based on a BDT. It is trained on the remaining background of atmospheric showers and a starting signal event sample of 600 GeV WIMPs annihilating to W^+W^-. The input variables used in the BDT describe the likelihood of the event to be starting within the fiducial volume, the event quality, the event brightness, and the zenith distance to the Galactic Center. The cut on the BDT score is optimized with respect to $Signal/\sqrt{Background}$. This final acceptance criterion reduces the background by more than one order of magnitude, retaining more than 50% of the signal.

The final event sample has a data rate of about 10 mHz in the declination band $\pm15°$ around the Galactic Center. The on-source region for a cut & count analysis is defined as $\pm15°$ in right ascension with respect to the Galactic Center. The sensitivity to the number of signal events in the on-source region is calculated from expected background, which is found by extrapolation from the number of off-source background events in the burn sample.

3 Sensitivities

Figure 3 shows the effective area for the DC-contained and DC-partial event selections, as well as for the IC event selection described above. Even though the effective area for the DC event selections is smaller when compared to the IC event selection, the sensitivity to the number of signal events is higher, and the adopted on-source region is larger in the DC event selections. This is reflected in the 90% confidence level sensitivities on $\langle\sigma_A v\rangle$, which were computed using the Feldman-Cousins approach [17].

Sensitivities for the low and high WIMP mass regimes resulting from the two independent analyses, are shown

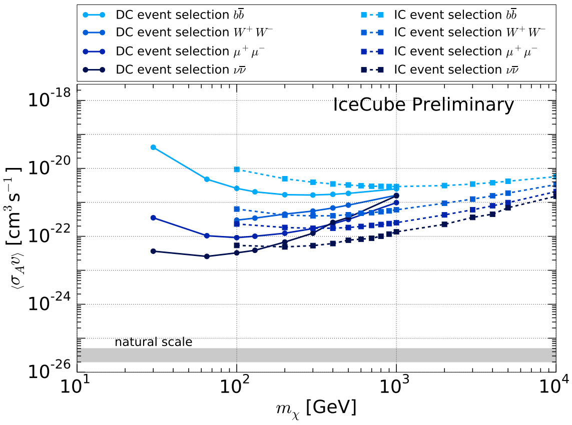

Figure 4: Sensitivities of the DeepCore low energy optimized (solid) and IceCube high energy optimized (dashed) independent analyses for different WIMP annihilation channels and WIMP masses.

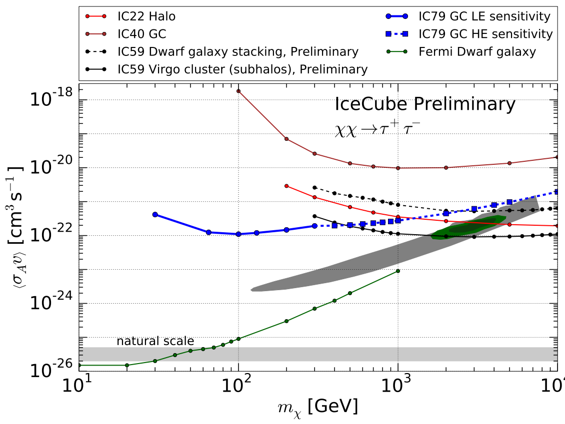

Figure 5: Sensitivity of this work (thick solid and dashed blue line) to the WIMP velocity-averaged self-annihilation cross-section into $\tau^+\tau^-$, compared to other analyses (see text).

in figure 4. Figure 5 shows the obtained sensitivities for annihilation to $\tau^+\tau^-$ in comparison to previous IceCube analyses: the IceCube-59 dwarf spheroid galaxy stacking and Virgo galaxy cluster search [18], the IceCube-40 Galactic Center analysis [19], and the IceCube-22 galactic halo analysis [20]. In addition, the preferred regions of the dark matter interpretation of the Pamela-excess (gray shaded region) with constraints from Fermi data (green shaded regions) [21] and the limits from Fermi [22] (green curve) are shown. The light-grey shaded band represents the natural scale at which WIMPs may appear as thermal relics.

For Galactic Center analyses, the largest model dependence comes from the chosen dark matter density profile. As described in section 1, the widely used NFW model has been chosen as a benchmark for the analyses presented here. Other models can be formulated based on the dark matter density profile kernel given by equation 1: the Moore and the Kravtsov model, which exhibits a cusped behavior in the central region, or has a flatter core region, respectively. The top panel of figure 1 shows the line-of-sight integral for each of the three models. The magnitude of the model-dependent variation of the presented sensitivities corresponds to the variation of the solid-angle-averaged value of the line-of-sight integral. It can be as large as one order of magnitude, compared to the NFW benchmark model.

4 Conclusions

Two approaches to search for annihilating dark matter in the Galactic Center have been presented, focusing on different WIMP mass regions. Both approaches use the nearly complete 79-string configuration of IceCube and 320 live days of data taken from 2010 to 2011. The sensitivity has been improved by up to 5 orders of magnitude for the $b\bar{b}$ channel of a 100 GeV WIMP mass when comparing with the previous Galactic Center analysis of IceCube-40 data [19]. Further, for the first time a Galactic Center analysis from IceCube has been extended to 30 GeV WIMP mass. The search for low-mass WIMPs benefits from the veto capabilities of large parts of the IceCube detector, while the intermediate mass range, between a few 100 GeV and a few TeV, is assisted by a larger fiducial volume definition, compared to DeepCore alone. At even higher WIMP masses, and thus higher neutrino energies, the constraint of a starting event selection as necessary veto against atmospheric muons reduces the effective area (see also dotted compared to solid and dashed lines in figure 3), which yields a weaker sensitivity.

References

[1] G. Bertone, D. Hooper and J. Silk, Phys. Rept., 405 (2005) 279.
[2] M. Drees and M. M. Nojiri, Phys. Rev. D, 47 (1993) 376.
[3] W. J. G. De Blok, A. Bosma and S. McGaugh, Mon. Not. R. Astron. Soc., 340 (2003) 657.
[4] J. Diemand, M. Kuhlen and P. Madau, Astrophys. J., 667 (2007) 859.
[5] L. Hernquist, Astrophys. J., 356 (1990) 359.
[6] J. F. Navarro, C. S. Frenk and S. D. M. White, Astro-phys. J., 462 (1996) 563.
[7] H. Yuksel et al., Phys. Rev. D, 76 (2007) 123506.
[8] B. Moore et al., Astrophys. J., 524 (1999) L19
[9] A. V. Kravtsov, A. A. Klypin, J. S. Bullock and J. R. Primack, Astrophys. J., 502 (1998) 48.
[10] T. Sjötrand, S. Mrenna and P. Skands, Comput. Phys. Commun., 178 (2008) 852.
[11] A. Achterberg et al., Astropart. Phys., 26 (2006) 155.
[12] R. Abbasi et al., Astropart. Phys., 35 (2012) 615.
[13] IceCube Coll., paper 0565 these proceedings.
[14] M. G. Aartsen et al., Phys. Rev. Lett., 110(13) (2013) 131302.
[15] A. Hoecker, P. Speckmayer, J. Stelzer, J. Therhaag, E. von Toerne and H. Voss, PoS ACAT 040 (2007).
[16] K. M. Gorski et al., Astrophys. J., 622 (2005) 759.
[17] G. J. Feldman and R. D. Cousins, Phys. Rev. D, 57 (1998) 3873.
[18] R. Abbasi et al., arXiv:1111.2738[hep-ex] (2011) (to be submitted to Phys. Rev. D).
[19] R. Abbasi et al., arXiv:1210.3557[hep-ex] (2012).
[20] R. Abbasi et al., Phys. Rev. D, 84 (2011) 022004.
[21] P. Meade, M. Papucci, A. Strumia and T. Volansky, Nucl. Phys. B, 831 (2010) 178.
[22] M. Ackermann et al., Phys. Rev. Lett., 107(24) (2011) 241302.